

EEDF MEASUREMENTS AND EXCITATION PROCESSES IN THE VICINITY OF A HELIUM DISCHARGE CONSTRICTION

S. Sobhanian and A. Muradov

Department of Physics, University of Tabriz, Tabriz, Islamic Republic of Iran

Abstract

Axial distributions of plasma and floating potentials, electron number density and the electron energy distribution function (EEDF) have been measured in the double layer (DL) region of an He discharge constriction. Excitation processes in the constriction region are studied. Using a linearization method for the nonstationary balance equations and choosing appropriate discharge conditions, the step excitation rate by electron impact for the $2^3S_1 \rightarrow 3^1D_2$ transition in He is determined.

Introduction

Double layers (DLs) in plasma have been studied by many authors. Interest in this problem arises from different important subjects, e.g. mono- and duoplasmatron ion sources [1], high intensity light emission sources [2], high current discharges [3], astrophysics experiments [4] and their laboratory modelling [5,6]. The DL represents the space charge region of order of tens to hundreds of Debye lengths. In this region, a sudden change in potential occurs due to space charge separation. The resulting electric field imparts additional energies to the electrons. These electrons are accelerated towards the higher potential side thereby changing the shape of electron energy distribution function (EEDF). Some changes occur in the ionization and excitation processes.

The simplest and more interesting (due to its applications) way of obtaining a DL in a plasma is to create sharp changes in the diameter of the positive column of a low pressure discharge [7,8,9]. In such discharge tubes, each part has its own potential distribution and it is only near the constriction region that the sharp changes occur in potential.

Keywords: Constriction region; Double layer; Step excitation

The DL formed at the change of discharge tube diameter has been studied in He [8]. EEDFs were calculated from the kinetic equation using the measured profile of potential when the momentum-transfer quasielastic collision frequency is significantly higher than the inelastic collision frequency and the characteristic scale is much longer than the electron mean free path. Double-humped distribution functions were obtained.

A double hump in EEDF due to the installation of an orifice has also been observed in an Hg-Ar mixture collision controlled positive column [9]. A one-dimensional model has been introduced to explain this EEDF by taking into account the absence of local equilibrium between the electrons and the electric field. A solution of the Boltzmann equation including the spatial derivative under the assumption of a rectangular-shaped electric field has successfully predicted a partial shift of low energy electrons to higher energies. It was shown that the regions of energy gain and energy loss are separated in space. This feature is a substantial deviation from the conventional positive column discharge where energy deposition and energy dissipation always go hand in hand.

Recently, the spatial variations of plasma parameters were detected in both axial and radial directions by

installing a mesh-grid in a homogeneous He positive column [10]. The EEDF has been measured and double-humped distributions were obtained. Spatial variation of radiation intensity was also detected by image reconstruction using a computerized tomography technique. The downstream variations of the EEDF were calculated from the kinetic equation solution using the Fourier transform method.

One can note that although the kinetics of electron acceleration and the physical properties of the constriction are well understood, to our knowledge excitation processes have not been completely studied. The special shape of the EEDF and different energy dependence of cross-sections of singlet and triplet levels may cause some peculiarities in excitation processes in the constriction region.

In the present paper, axial distributions of plasma and floating potential, electron number density and the EEDF have been measured in the DL region in the He discharge constriction. Excitation processes in the constriction region are studied. Using the linearization method for the nonstationary balance equation system [11] and choosing appropriate discharge conditions, the step excitation rate in He for the $2^3S_1 \rightarrow 3^1D_2$ transition is determined.

Experimental Arrangement and Results of Stationary Measurements

Experiments were carried out in the positive column of a hot cathode discharge in helium. The discharge tube is composed of two cylindrical glass tubes of different diameters, 55 and 18 mm (Fig. 1). The discharge was maintained between a directly heated tungsten filament in

the wide part of the tube and a conic-shaped nickel anode placed in the movable narrow part of the tube. A movable Langmuir probe which provides radial distribution measurements of plasma parameters is placed into the discharge tube. The DL position with respect to the probe or monochromator's slit could be changed by moving the anode, placed in the narrow part of the tube, with the help of a magnet. The measurements were carried out in helium at a pressure range of 0.06-0.6 torr in the discharge current range from 20 to 600 mA.

The EEDF and electron number density were measured by the method of second derivative of the probe characteristic [12]. The amplitude modulated RF signal is superimposed on probe bias. The amplitude of modulating harmonic of probe current is plotted versus the probe bias voltage. This curve represents the second derivative of probe characteristic and is proportional to the EEDF. Plasma potential was determined at zero value of second derivative. The electron number density was determined from the probe current at plasma potential. Spectral line intensities were measured in the transverse direction without taking into account the radial distribution of plasma parameters.

The discharge constriction region, axial distribution of electron number density, plasma potential and floating potential distributions at discharge current value 200 mA are shown in Figure 2. As seen from this figure, near the constriction, electron density increases sharply first and then falls to density levels of the narrow part undergoing some oscillations. Electron density maximum is shifted as a whole towards the anode side with respect to the potential drop (maximum electric field). Electrons are

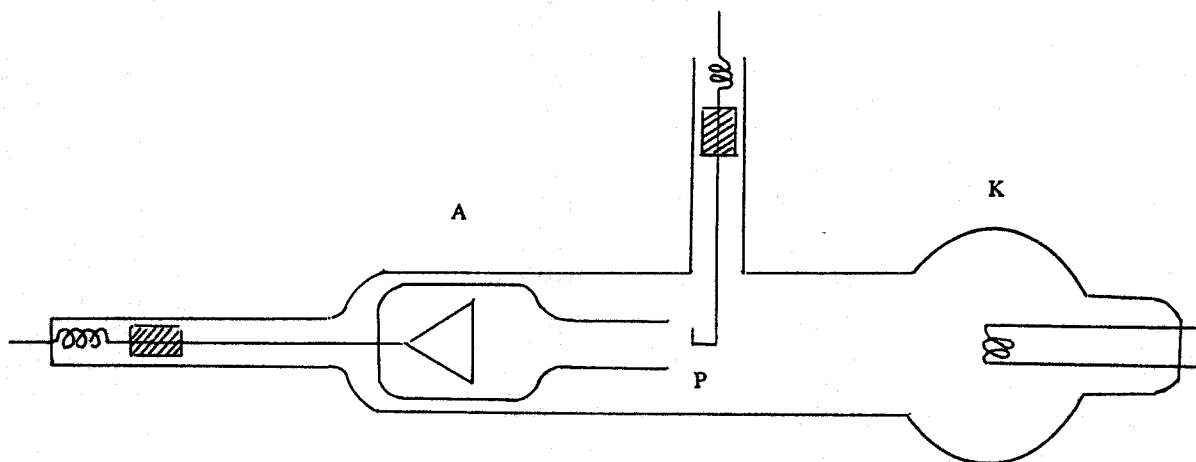


Figure 1. Discharge tube constriction scheme. A-movable conic-shaped anode, K-cathode, P-movable Langmuir probe.

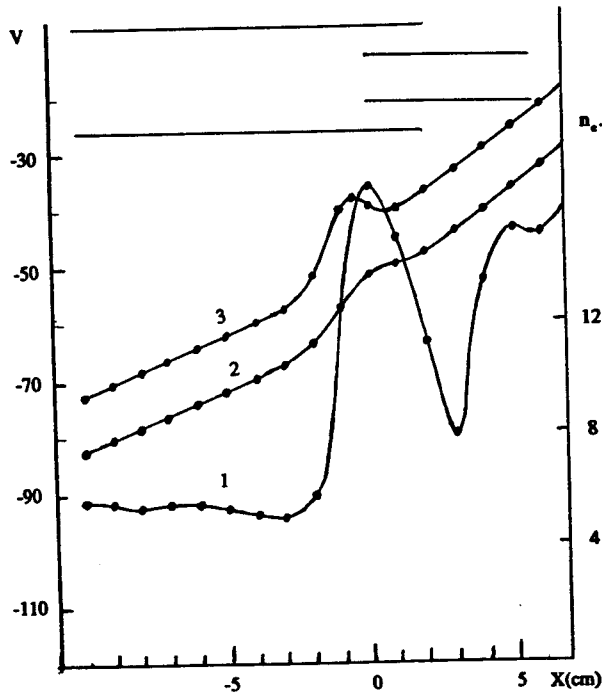


Figure 2. Distributions of plasma parameters as a function of distance from the constriction edge: 1. Electron number density, 2. Ion plasma potential, 3. Floating potential. Constriction region is shown in the upper section of the figure.

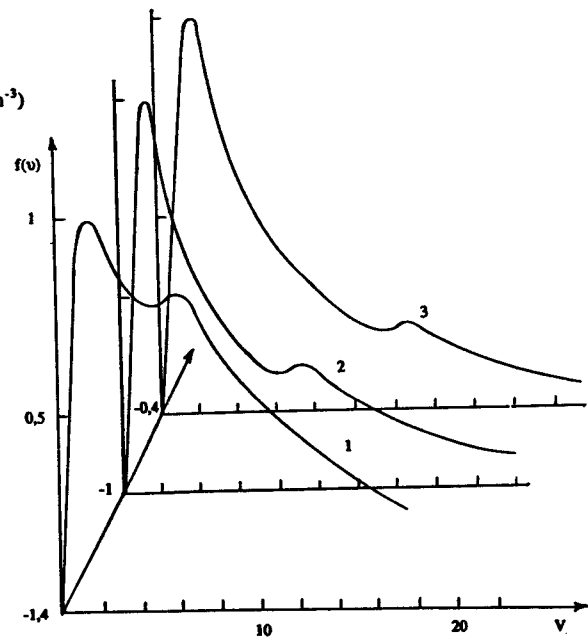


Figure 3. EEDF measured at distances of 14 (curve 1), 10 (curve 2) and 4 mm (curve 3) from the constriction edge

accelerated through the DL and gain additional energies. The amount of ionization is thus increased and this will result in the increase of charged particles densities towards the higher potential region. Axial distribution of plasma potential V_p and floating potential V_0 are also shown in the same figure. The changes in difference between V_p and V_0 are due to the significant changes in the EEDF shape.

The DL is a spherical segment formed near the constriction and the accelerated electrons are focused towards the narrow part. Radial distributions of charged particles in the vicinity of the constriction are significantly narrower than those for the regions far from the DL.

The EEDF and potential distribution measurements at different discharge currents showed no changes in potential drop and the EEDF shape for the current range of 20 to 600 mA. Accordingly, the increase in discharge current leads to the increase of absolute ion and electron densities, while the EEDF shape and excitation regimes remain the same. The EEDF measured at distances of 14, 10, and 4 mm from the constriction edge towards the cathode side is shown in Figure 3. Additional maximum in the EEDF corresponds to the electrons accelerated in the DL. As one can see, a shift in the probe position towards the anode leads to a shift of the additional maximum towards the higher energies and to a decrease in its value.

Numbers of excitations of triplet and singlet levels were calculated from the measured EEDF and cross-sections data [14]. Results of calculations for the 3^3P_1 and 3^1P_1 levels are shown in Figure 4 (points).

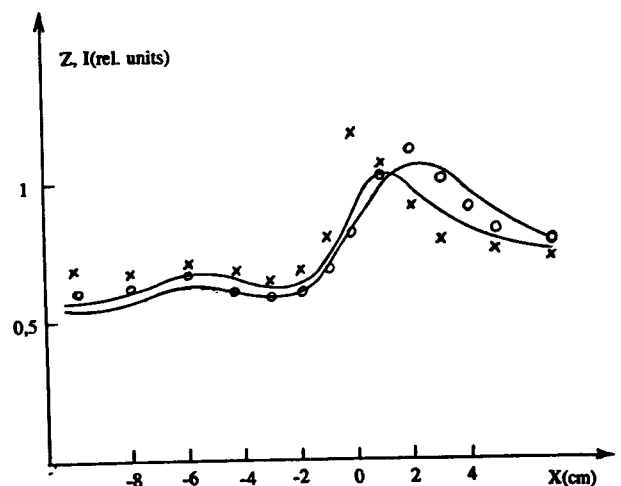


Figure 4. Axial distributions of relative intensities of spectral lines: curve (1), $\lambda = 388.9$ nm and curve (2), $\lambda = 501.6$ nm. Crosses (X) and open circles (O) represent the calculated numbers of excitations for the 3^3P_1 and 3^1P_1 levels, respectively.

Axial distributions of relative intensities of spectral lines $\lambda = 388.9 \text{ nm}$ and $\lambda = 501.6 \text{ nm}$ are shown on the same figure. As is seen, these curves are shifted relative to each other and their intensities reach their maximum at different distances from the constriction. The change in excitation regimes of triplet and singlet levels results from the shift in the second maximum position on the EEDF and from the different energy dependencies of the corresponding level's cross-sections.

The discrepancy between calculation and measured intensities can be explained by the fact that the radial distribution of plasma parameters has been neglected. This would give the difference between the calculated intensities at the tube centre and the measured intensities across the tube cross-section (integrated along the diameter). Similar changes were observed in the population relations for other triplet and singlet levels taking into account changes due to their different threshold energies. Thus, it is possible to create a local partial preferable selective population of some levels using the changes in the excitation rates of different type levels in the positive column constriction.

Determination of Step Excitation Rate of He in Nonstationary Discharge Constriction

The existence of a shifting hump on the EEDF and changes in excitation rates of different type levels can be used for simple determination of step excitation rates. These rates and corresponding cross-sections are very important in atomic spectroscopy and plasma physics. There is little experimental data on this subject and calculated theoretical results are commonly used for different studies. Such a calculation was performed and reported recently for He [15].

Let us consider the system of balance equations for two levels. One of them is metastable (m) which is excited only directly by electron impact. The other one is excited not only directly, but also by step excitation from the metastable levels. The balance equations may be written as:

$$\frac{dN_m}{dt} = N_0 n_e \alpha_{om} - (n_e \beta_m + \tau_m^{-1}) N_m \quad (2)$$

$$\frac{dN_k}{dt} = N_0 n_e \alpha_{ok} + N_m n_e \alpha_{mk} - N_k A_k \quad (3)$$

Here N_0 and n_e are respectively normal atom and electron number densities, N_m and N_k are populations of considering levels, α_{om} and α_{ok} are direct excitation rates, α_{mk} and β_m are step excitation and loss rate coefficients for metastable atoms due to electron impact, τ_m is the diffusion

time of metastable atoms to the walls of tube and A_k is the spontaneous transition probability. It is assumed that metastable atoms are lost by means of electron impact transition to neighbouring levels and by diffusion to the discharge tube walls. The second level is lost as the result of spontaneous transition to lower levels.

Let us assume plasma parameters oscillations in the form of:

$$n_e(t) = n_0 + n_1 e^{i\omega t}; N_m(t) = N_{m0} + N_{m1} e^{i\omega t}; N_k(t) = N_{k0} + N_{k1} e^{i\omega t} \quad (4)$$

Here subscripts 0 and 1 denote the unperturbed values and complex amplitudes of plasma parameters.

If $\ln_1 \ll n_0, \ln_{m1} \ll N_{m0}, \ln_{k1} \ll N_{k0}$, the equations (2,3) are linearized as:

$$i\omega N_{m1} = N_0 n_1 \alpha_{om} - (n_0 \beta_m + \tau_m^{-1}) N_{m1} - n_1 \beta_m N_{m0} \quad (5)$$

$$i\omega N_{k1} = N_0 n_1 \alpha_{ok} + (N_{m0} n_1 + N_{m1} n_0) \alpha_{mk} - N_{k1} A_k \quad (6)$$

Equations (5) and (6) represent the complex amplitudes of oscillating plasma parameters. At $\omega \rightarrow 0$ these equations are simplified as:

$$N_0 n_1 \alpha_{om} + (n_0 \beta_m + \frac{1}{\tau_m}) N_{m1} - n_1 \beta_m N_{m0} = 0 \quad (7)$$

$$N_0 n_1 \alpha_{ok} - (N_{m0} n_1 + N_{m1} n_0) \alpha_{mk} - N_{k1} A_k = 0 \quad (8)$$

From these equations one can obtain:

$$\eta_{IK} = \eta_n \left(1 + \frac{N_{m0}^2}{N_0 \alpha_{om} I_{k0} \tau_m} \alpha_{mk} \right) \quad (9)$$

Here $I_{k0} = N_{k0} A_{k0}$ and $\eta_{IK} = \frac{N_{k1}}{N_{k0}}$, $\eta_n = \frac{n_1}{n_0}$ are modulation depths of spectral line intensity and electron density.

As is seen from Equation 9, one can obtain α_{mk} by plotting $\eta_I - \eta_n$ versus η_n . N_{m0} , I_{k0} and N_0 are measurable quantities, and direct excitation rate α_{om} and diffusion time τ_m can be calculated.

Electron density measurements for different discharge currents and at different points showed that at low frequencies electron density modulation depth is equal to the discharge current modulation depth in a wide range of discharge currents. Thus, in Equation (9), η_n is replaced by η_I for simplifying purposes.

In the stationary case of Equation 2 at low discharge currents and low electron densities, only diffusion to the tube's wall remains in the metastable atom's loss term. Due to the proportionality of metastable atom creation

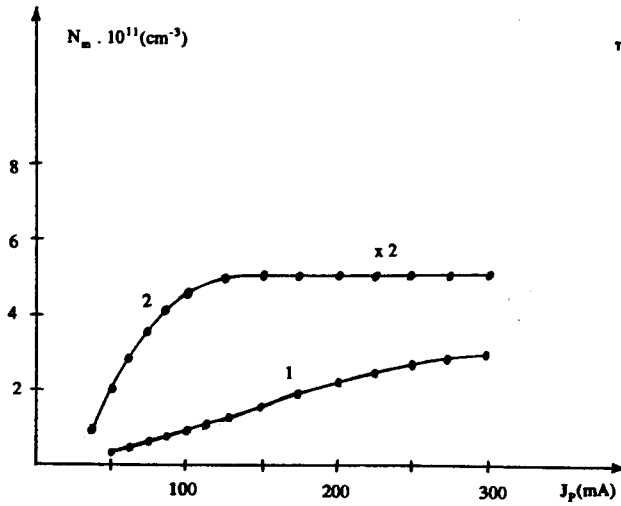


Figure 5. The dependence of 2^1S_0 (curve 1) and 2^3S_1 (curve 2) level populations on discharge current at 12 mm from the constriction edge

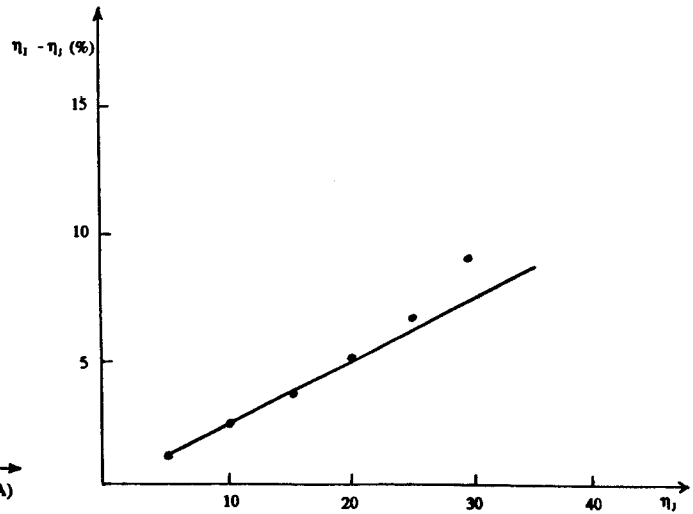


Figure 6. The dependence of $\eta_1 - \eta_2$ on η_1 for the spectral line $\lambda = 667.8$ nm. $P = 0.3$ torr, $J_p = 100$ mA. Current modulation frequency $\nu = 63$ Hz.

Table 1.

J_p (mA)	P(torr)	$N_0(1^1S_0)cm^{-3}$	$N_{mo}(2^3S_1)cm^{-3}$	$\alpha_{om}(1^1S_0 \rightarrow 2^3S_1)cm^3s^{-1}$
100	0.3	$9.6 \cdot 10^{15}$	$9.1 \cdot 10^{11}$	$3.5 \cdot 10^{-11}$

$I_{ko}(cm^{-3}s^{-1})$	$\tau_m(s)$	$\alpha_{mk}(exp)cm^3s^{-1}$	$\alpha_{mk}(calc.)cm^3s^{-1}$
$4 \cdot 10^{14}$	$8 \cdot 10^{-4}$	$9 \cdot 10^{-9}$	$1.4 \cdot 10^7$

rate with electron density, N_m increases linearly by increasing discharge current. At high electron densities the diffusion term can be neglected, the gain and loss rates of metastable atoms become proportional to electron density, and N_m remains invariant with respect to the increase of discharge current.

The dependence of 2^3S_1 and 2^1S_0 level populations measured at a distance 12 mm to the cathode side from the constriction edge is shown in Figure 5. Measurements of populations were performed on the basis of $\lambda = 388.1$ nm and $\lambda = 546.6$ nm line absorption. It can be seen that the 6^3P_0 level population is saturated at 300 mA and that of 2^3S_1 level at $J_p = 100$ mA.

To determine the step excitation rate, the discharge current was modulated at a frequency 63 Hz. This frequency was lower than all characteristic frequencies in the discharge and satisfies the $\omega \rightarrow 0$ condition. To obtain appreciable modulation depth of 2^3S_1 level population

and to reach the stage where its role on step excitation at current modulated regime is more significant, discharge currents were taken within the 100 mA range.

The dependence of $\eta_1 - \eta_2$ on η_1 for $\lambda = 667.8$ nm line at $J_p = 100$ mA, $P = 0.3$ torr is shown in Figure 6. Other quantities in Equation 9 are represented in Table 1. The value of α_{mk} for the transition $2^3S_1 \rightarrow 3^1D_2$ determined from Equation 9 is also shown in this table. The calculated rate of this transition using the first Born approximation [16] is given in the last column.

As one can see, the experimental value for the transition rate is higher than the calculated one. This discrepancy may be the result of neglecting transitions from 2^1S_0 , 2^3P and 2^1P_1 levels. These levels, which don't have appreciable contribution to step excitation in the stationary case, can not reach saturation. They have a high modulation depth for a wide range of discharge currents. Consequently, they could have considerable contribution in the current

modulated regime. Furthermore, the transition rate calculations were performed for the Maxwellian distribution, while the measured EEDFs were double-humped distributions very different from the Maxwellian case. One can conclude that the EEDF is not completely Maxwellian near the constriction region.

References

1. Lavrov, B.P. and Simonov, V.Y. *Journ. of Techn. Phys.*, **48**, (8), 1744, (1978).
2. Lavrov, B.P. and Shitashka, L.P. *Optical and Mechanical Industry*, (11), 58, (1979).
3. Lutsenko, E.I., Sereda, N.D. and Kontsevov, L.M. *Journ. of Tech. Phys.*, **45**, 789, (1975).
4. Block, L. *Astrophys. Space Sci.*, **55**, 59, (1978).
5. Torven, S. and Lindberg, L. *J. Phys. D. Appl. Phys.*, **13**, 2285, (1980).
6. Raadu, M. and Carlquist, P. *Astrophys. Space Sci.*, **74**, 189, (1981).
7. Anderson, D. *J. Phys. D. Appl. Phys.*, **10**, 1549, (1977).
8. Husseinov, T.H. and Muradov, A.H. *Journ. of Techn. Phys.*, **61**, (5), 130, (1991).
9. Godyak, V. and Lagushenko, R. *Maya J. Phys. Rev. A.*, **38**, (4), 2044, (1988).
10. Ohe, K. and Yamada, H. *J. Phys. D. Appl. Phys.*, **27**, 756, (1994).
11. Muradov, A.H. *Radiophysics*, **31**, (6), 763, (1988).
12. Vorobyova, N.A., Kagan, Y.M. and Milenin, V.M. *Journ. of Techn. Phys.*, **34**, 2079, (1964).
13. Kaptsov, N.A. *Electricity in gases and vacuum*. M.L. (1947).
14. Zapesochniy, I.P. and Feltsan, P.V. *Opt. and Spect*, **18**, 911, (1965).
15. Shevelko, V.P. and Tawara, H. Cross-sections for Electron-impact induced transitions between excited states in He. NIFS-DATA-28, Nagoya, (1995).
16. Vaynshtein, L.A., Sobelman, I.I. and Yukov, E.A. Cross-sections of atoms and ions. Nauka, (1974).